microRNA -378a-3p Restrains the Proliferation of Retinoblastoma Cells but Promotes Apoptosis of Retinoblastoma Cells via Inhibition of FOXG1

Chao Zhang[1] and Shuai Wu[2]

[1]Department of Strabismus & Pediatric Ophthalmology, The Second Hospital of Jilin University, Changchun, P.R. China
[2]Department of Ophthalmology, The Second Hospital of Jilin University, Changchun, P.R. China

Correspondence: Shuai Wu, Department of Ophthalmology, The Second Hospital of Jilin University, No. 218, Ziqiang Street, Nanguan District, Changchun 130000, Jilin Province, P.R. China; wswushuai2018@126.com.

Received: June 11, 2019
Accepted: January 14, 2020
Published: May 19, 2020

Citation: Zhang C, Wu S. microRNA -378a-3p restrains the proliferation of retinoblastoma cells but promotes apoptosis of retinoblastoma cells via inhibition of FOXG1. *Invest Ophthalmol Vis Sci.* 2020;61(5):31. https://doi.org/10.1167/iovs.61.5.31

Purpose. More recently, literature has emerged providing findings about the novelty of microRNAs (miR)-targeted therapeutics in the treatment of retinoblastoma (RB). The prime objective of this study was to identify the potential role of miR-378a-3p and its regulation in RB cells via forkhead box G1 (FOXG1).

Methods. The expression of miR-378a-3p and FOXG1 in the clinical RB tissues was determined using RNA quantitation and Western blot assays. The interaction between miR-378a-3p and FOXG1 was identified using dual luciferase reporter gene assay. The potential effects of miR-378a-3p on the RB cell biological processes were evaluated by conducting gain- and loss-of-function studies of miR-378a-3p and FOXG1, followed by cell viability, cell cycle progression, and apoptosis measurements. Furthermore, experiments were performed in nude mice to assess its effects on tumor formation.

Results. miR-378a-3p was poorly expressed, whereas FOXG1 was highly expressed in RB tissues and cells. miR-378a-3p bound to the FOXG1 3′ untranslated region and negatively modulated its expression. The overexpression of miR-378a-3p was found to decrease RB cell viability and to promote cell apoptosis in vitro, whereas overexpressed FOXG1 reversed the regulatory effects of miR-378a-3p on RB cellular behaviors. In nude mice, the restoration of miR-378a-3p by miR-378a-3p agomir was shown to play a role in the reduction of tumor volume and size relative to nude mice injected with negative control-agomir.

Conclusions. Our findings identified that increased miR-378a-3p exerted an inhibitory effect on RB cell proliferation by targeting FOXG1, suggesting the role of miR-378a-3p as a novel therapeutic target for RB.

Keywords: retinoblastoma, microRNA-378a-3p, forkhead box G1, apoptosis, proliferation, cell cycle progression

Retinoblastoma (RB) is a childhood neoplasm that occurs during the development of the retina.[1] Patients suffering from RB commonly present with an abnormal white leukocoria or strabismus.[2] The inactivation of both copies of the *RB1* gene is the predominant initiating genetic lesion in RB and is rate limiting for tumorigenesis.[3] Local delivery of chemotherapy by intra-arterial and intravitreal administration has become the leading eye-sparing treatment in the past decade in Western countries.[4] Nevertheless, the risk of immunogenicity and the hazardous integration of chemotherapeutic agents such as melphalan and curcumin in healthy cells is inevitable.[5,6] Importantly, the implication of microRNAs (miRNAs) in chemotherapy has been recognized.[7,8] Sage and VenturaHYPERLINK[9] have described in a previous study that the dysregulation of several miRNAs is involved in a several of stages of RB and those miRNAs might serve as the potential diagnostic and therapeutic biomarkers for RB, providing insights into the advancement in treatment approaches.

Several miRNAs have been identified as tumor suppressors for RB, where RB tumorigenesis can be inhibited by the overexpression of miR-125a-5p[10] and miR-183[11] in vitro. In addition, miR-378a-3p has been documented to be involved in the metastasis of melanoma.[12] miR-378a-3p can potentially impede the progression of esophageal squamous cell carcinoma by negatively targeting Rab10, as shown in a previous study.[13] However, the specific role of miR-378a-3p and its underlying mechanism in the onset and progression of RB have not been elucidated yet. The prediction results obtained from TargetScan database revealed that miR-378a-3p could target FOXG1, hence leading to the hypothesis that miR-378a-3p might exert its function through regulating FOXG1. It has been shown that forkhead box G1 (FOXG1) is highly expressed in glioblastomas and promotes the growth of glioblastomas.[14] FOXG1 is a nuclear cell transcription factor involved in the development of the forebrain and has been implicated in in neurogenesis and cancer pathology.[15] It has been demonstrated that FOXG1 has the abil-

ity to promote the onset and progression of glioblastoma.[16] Also, enhanced survival has been observed in intracerebellar mice xenografts treated with medulloblastoma cells bearing silencing of FOXG1,[17] but whether FOXG1 could exert the function in RB has been rarely studied. Therefore, the present study was designed with an objective of investigating the interaction between miR-378a-3p and FOXG1 as well as their functions in RB.

Methods

Ethics Statement

The experiment was approved by the Ethics Committee of The Second Hospital of Jilin University. All participants provided the signed written informed consent documents and the experimental procedures were performed in compliance with the Declaration of Helsinki. All animal experiments were performed in strict accordance to the recommendations from the Guide for the Care and Use of Laboratory Animals of the National Institutes of Health.

Microarray-Based Gene Expression Profiling

Screening of the potential miRNAs that could regulate FOXG1 were performed using TargetScan database (www.targetscan.org/vert_71/), miRSearch database (www.exiqon.com/miRSearch), and miRNA database (www.microrna.org/microrna/home.do?tdsourcetag=s_pcqq_aiomsg).

Patient Enrollment

Twenty-eight patients with RB (12 males and 16 females) with the mean age of 2.9 years diagnosed at The Second Hospital of Jilin University between March 2017 and May 2018 were enrolled in this study. No patient had received chemoradiotherapy before the operation. Subsequently, RB tissues and the matched normal retinal tissues were collected from the enucleation. All samples were diagnosed by two pathologists for further study.

Cell Culture

RB cell lines (Y79, SO-Rb50, SO-Rb70) (National Infrastructure of Cell Line Resource, Beijing, China; www.cellresource.cn/) and human retinal astrocyte cell line HRA (Shanghai Zhongqiaoxinzhou Biotech Co., Ltd., Shanghai, China) were enrolled in our study. Western blot analysis was conducted to determine the RB cell lines that presented with the highest FOXG1 expression, which were then selected for subsequent experiments.

Cell Transfection

RB cell lines were transfected with miR-378a-3p mimic, miR-378a-3p inhibitor, overexpressed FOXG1 plasmid (oe-FOXG1), short hairpin targeting FOXG1 (sh-FOXG1), or their negative controls (NC mimic, sh-NC and oe-NC) to alter the expression of miR-378a-3p and FOXG1. The RB cells were seeded into 12-well plates at a cell density of 3×10^5 cells/mL per well. When cell confluence reached about 80%, the cells were transfected according to the protocol provided on the Lipofectamine 2000 Kit (11668019, Thermo Fisher Scientific, Rockford, IL).

Table. Primer Sequences for RT-qPCR

Primer	Sequence
miR-378-3p	F: 5'-CTCAACTGGTGTCGTGGAGT-3'
	R: 5'-GGGACTGGACTTGGAGTC-3'
U6	F: 5'-CTCGCTTCGGCAGCACA-3'
	R: 5'-AACGCTTCACGAATTTGCGT-3'

F, forward; R, reverse.

RT-qPCR

TRIzol reagent (Invitrogen Inc., Carlsbad, CA) was used for total RNA extraction from RB tissues and cells using TRIzol reagent (Invitrogen). RNA concentration and purity were then determined using a NanoDrop 2000 microultraviolet spectrophotometer (1011U, NanoDrop Technologies, Wilmington, DE). Next, the RNA was reversely transcribed into cDNA in accordance with the manufacturer's instructions of TaqMan MicroRNA Assays Reverse Transcription Primer (4427975, Applied Biosystems, Carlsbad, CA). The miR-378a-3p primer was designed and synthesized by Takara Bio Inc. (Otsu, Shiga, Japan) (Table). The real-time qPCR was performed with ABI7500 qPCR instrument (7500, ABI Company, Oyster Bay, NY). The fold changes were calculated using the relative quantification ($2^{-\Delta\Delta Ct}$) method with U6 as an internal control.[16]

Western Blot Analysis

Western blot analysis was conducted following the protocol provided by Liu et al.[18] The antibodies used were the primary antibody, rabbit monoclonal antibody to FOXG1 (1:1000, ab196868), rabbit antibody to bcl-2–associated X protein (Bax, 1:1000, ab32503), rabbit antibody to B-cell chronic lymphocytic leukemia/lymphoma 2 (Bcl-2, 1:2000, ab182858), rabbit antibody to CCND2 (1:1000, ab207604), and rabbit antibody to glyceraldehyde-3-phosphate dehydrogenase (internal reference, ab9485, 1:2500) and the secondary antibody, horseradish peroxidase-conjugated goat anti-rabbit IgG H&L (ab97051, 1:2000, Abcam Inc., Cambridge, UK) for 1 hour.

Cell-Counting Kit 8 (CCK-8) Assay

The RB cell viability was detected by CCK-8 assay (CK04, Dojindo Laboratories, Kumamoto, Japan) using cell counter kit. The cells were incubated with 10 µL CCK-8 reagent at 37°C for 3 hours at 0, 24, 48, and 72 hours after transfection, the cells were incubated with 10 µL CCK-8 reagent at 37°C for 3 hours. Then, the optical density values of each well were measured at 450 nm wavelength on a microplate reader.

TUNEL

RB cells in the logarithmic growth phase with cell density of 1×10^6 cells/mL were seeded on a cover glass in 6-well plates. The 1in Situ Cell Death Detection Kit (11684795910, Roche Diagnostics, Basel, Switzerland) was applied for cell apoptosis assessment in strict accordance with the protocol. Finally, five high-power visual fields were randomly selected and the number of TUNEL-positive cells was counted.

Investigative Ophthalmology & Visual Science

Flow Cytometry

After 48 hours of transfection, the cells in each group underwent centrifugation and re-suspension with PBS to a cell density of 1×10^6 cells/mL, followed by fixation with 70% cold ethanol at 4°C for 4 hours, after which the ethanol was then removed through centrifugation. The cells were suspended in 40 µL phosphate sodium citrate, and allowed to stand at room temperature for 30 minutes. Next, the cells were resuspended with 100 µL PBS after centrifugation, followed by the addition with RNaseA to a concentration of 50 mg/mL. The cells were then incubated at 37°C for 1 hour and stained with 50 µL propidium iodide solution (50 mg/mL) avoiding light exposure at 4°C for 30 minutes. Finally, flow cytometer (FACScalibur, Becton Dickinson, Franklin Lakes, NJ) was used for the analysis of the cell cycle distribution.

After 48 hours of transfection, the cells were centrifuged and then resuspended with PBS at 3×10^5 cells/mL. A total of 500 µL cell suspension was incubated at room temperature for 15 minutes with 5 µL Annexin-V-fluorescein isothiocyanate and 10 µL propidium iodide. Cell apoptosis was detected using the flow cytometer (FACScalibur, Becton Dickinson).

Dual Luciferase Reporter Gene Assay

Based on the results obtained from the TargetScan database (www.targetscan.org/vert_71/), miR-378a-3p was predicted as the miRNA that could potentially regulate FOXG1. The cDNA fragment of FOXG1 3′-untranslated region containing miR-378a-3p binding site was inserted into pmirGLO vector. The cDNA fragment of FOXG1 3′-untranslated region with mutated binding site was constructed by a site-directed mutagenesis method and then inserted into the pmirGLO vector. The inserted sequence was confirmed to be correct by sequencing. PmirGLO-FOXG1 or pmirGLO-mutant FOXG1 recombinant vector were cotransfected with miR-378a-3p mimic or NC mimic into HEK293T cells using the liposome transfection method, respectively, which was followed by a 48-hour incubation. After that, the cells were collected and lysed. An amount of 100 µL lysate supernatant was added with 100 µL Renilla luciferase detection reagent in order to detect the Renilla luciferase activity. In addition, 100 µL lysate supernatant was mixed with Firefly luciferase detection reagent to determine the activity of Firefly luciferase. A multifunctional microplate reader SpectraMax M5 was used to measure the activity of Renilla luciferase and Firefly luciferase, respectively.

Xenograft Tumor in Nude Mice

Twelve specific-pathogen-free male BALB/c nude mice aged 6 weeks and weighing 15 to 18 g were purchased from Shanghai SLAC Laboratory Animal Co., Ltd. (Shanghai, China). The Y79 cells in the logarithmic growth phase were dispersed into cell suspension at a cell density of 1×10^7 cells/mL. The prepared Y79 cell suspension (1 mL) that was prepared was subcutaneously injected into left armpit of the nude mice with a syringe.[19,20]

When the tumor tissue size reached 50 mm^3, the nude mice were injected with miR-378a-3p agomir or NC agomir at a dosage of 10 nmol/mouse once every 5 days for a total of 5 weeks, 6 mice per treatment group. Five weeks later, the mice were euthanized, followed by the extraction of subcutaneous xenotransplanted tumors with the tumor weight recorded. Finally, the tumor tissues were extracted and analyzed by Western blot analysis.

Statistical Analysis

All statistical analyses were conducted using the SPSS 21.0 statistical software (IBM Corp., Armonk, NY, USA). Measurement data were expressed as mean ± standard deviation. Comparisons between RB and matched normal retinal tissues were conducted using paired *t*-test. Comparisons of normally distributed data between two groups were analyzed by independent sample *t*-test. Data among multiple groups were analyzed by one-way ANOVA, followed by Tukey's post hoc test. A P value of less than 0.05 was considered to be statistically significant.

Results

FOXG1 Expresses Highly in RB Tissues and Cells

To reveal the role of FOXG1 in RB cells, Western blot analysis was performed to examine the expression of FOXG1. The results revealed a remarkable increase in FOXG1 expression in the RB tissues compared with the matched normal retinal tissues (Figs. 1A, B). Compared with the HRA cell line, the RB cell lines Y79, SO-Rb50, and SO-Rb70 presented with significantly elevated FOXG1 expression (Figs. 1B, C). These findings suggested that FOXG1 was overexpressed in RB.

Downregulated FOXG1 Inhibits Cell Cycle Progression and Facilitates Cell Apoptosis in RB

The expression of FOXG1 in Y79 and SO-Rb50 cell lines was altered by transfection with oe-FOXG1, sh-FOXG1#1, or sh-FOXG1#2, the transfection efficiency of which was detected by Western blot analysis. The data showed a significant increase in the expression of FOXG1 in Y79 and SO-Rb50 cells transfected with oe-FOXG1, whereas the FOXG1 expression was drastically lowered following transfection with either sh-FOXG1#1 or sh-FOXG1#2, as shown in Figure 2A and Supplementary Figure S1A. Next, the protein expression of apoptosis-related proteins Bax and Bcl-2, as well as CCND2 in Y79 and SO-Rb50 cells that were transfected with oe-FOXG1 and sh-FOXG1 was measured using Western blot analysis. The results showed that the protein expression of Bcl-2 and CCND2 was upregulated, and the protein expression of Bax was inhibited in Y79 and SO-Rb50 cells transfected with oe-FOXG1, which was opposite to the changes in Y79 and SO-Rb50 cells that were transfected with sh-FOXG1 (Fig. 2B, Supplementary Fig. S1B). CCK-8 assay was used for the assessment of cell viability, which was found to be remarkably elevated after transfection with oe-FOXG1, and reduced after transfection with sh-FOXG1 (Fig. 2C, Supplementary Fig. S1C). Furthermore, TUNEL assay data showed that Y79 and SO-Rb50 cells had lower apoptotic ability after oe-FOXG1 transfection, and elevated apoptotic ability after transfection of sh-FOXG1 (Fig. 2D, Supplementary Fig. S1D). The cell cycle and cell apoptosis were determined by flow cytometry, and the results revealed that the overexpressed FOXG1 led to decreased proportion of cells at G0/G1 phase, increased proportion of cells at S phase, and reduced apoptosis rate of RB cells; silencing FOXG1 resulted in increased proportion of cells at G0/G1 phase, lowered proportion of cells at S phase, and elevated

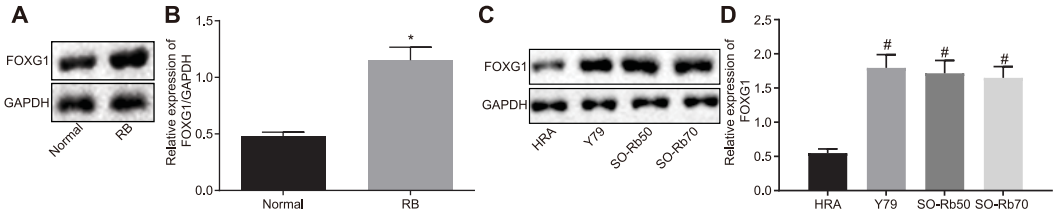

Figure 1. FOXG1 is expressed at a high level in RB tissues and cells. (**A** and **B**) Western blot analysis of FOXG1 protein expression in RB tissues and matched normal tissues ($n = 28$) normalized to glyceraldehyde-3-phosphate dehydrogenase (GAPDH). Comparisons between two groups were analyzed by paired *t*-test. * $P < 0.05$ versus matched normal tissues. (**C** and **D**) Western blot analysis of FOXG1 in human retinal astrocyte cell line HRA and RB cell lines Y79, SO-Rb50, and SO-Rb70 normalized to GAPDH. Statistical values were measurement data and expressed as mean ± standard deviation. One-way ANOVA was used for comparisons of data among multiple groups, followed by a Tukey's post hoc test. # $P < 0.05$ versus the HRA cells. The experiment was repeated three times independently.

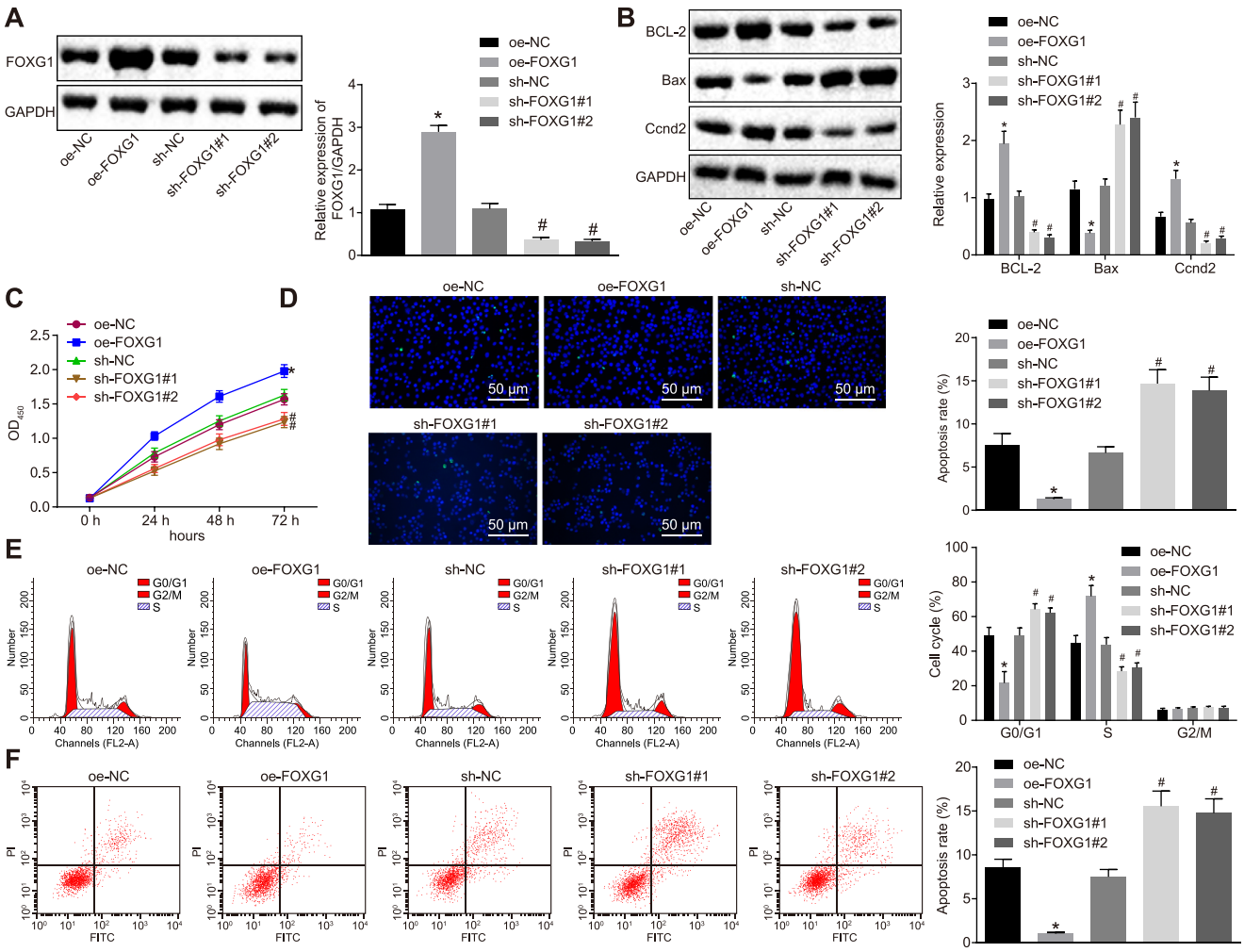

Figure 2. Silencing of FOXG1 inhibits Y79 cell growth and facilitates Y79 cell apoptosis in RB. Y79 cells were treated with oe-FOXG1, sh-FOXG1#1 or sh-FOXG1#2. (**A**) Western blot analysis of FOXG1 protein expression after oe-FOXG1 and sh-FOXG1 transfection normalized to glyceraldehyde-3-phosphate dehydrogenase (GAPDH). (**B**) Western blot analysis of Bcl-2, Bax, and CCND2 proteins normalized to GAPDH. (**C**) Cell viability detected by CCK-8 assay. (**D**) Cell apoptosis tested by TUNEL assay (original magnification ×200×). (**E**, **F**) Cell cycle distribution and apoptosis assessed by flow cytometry. Statistical values were measurement data and expressed as mean ± standard deviation. Independent *t*-test was used to compare the data between two groups. * $P < 0.05$ versus the oe-NC-transfected Y79 cells. # $p < 0.05$ versus the sh-NC-transfected Y79 cells. The experiment was repeated three times independently.

Investigative Ophthalmology & Visual Science

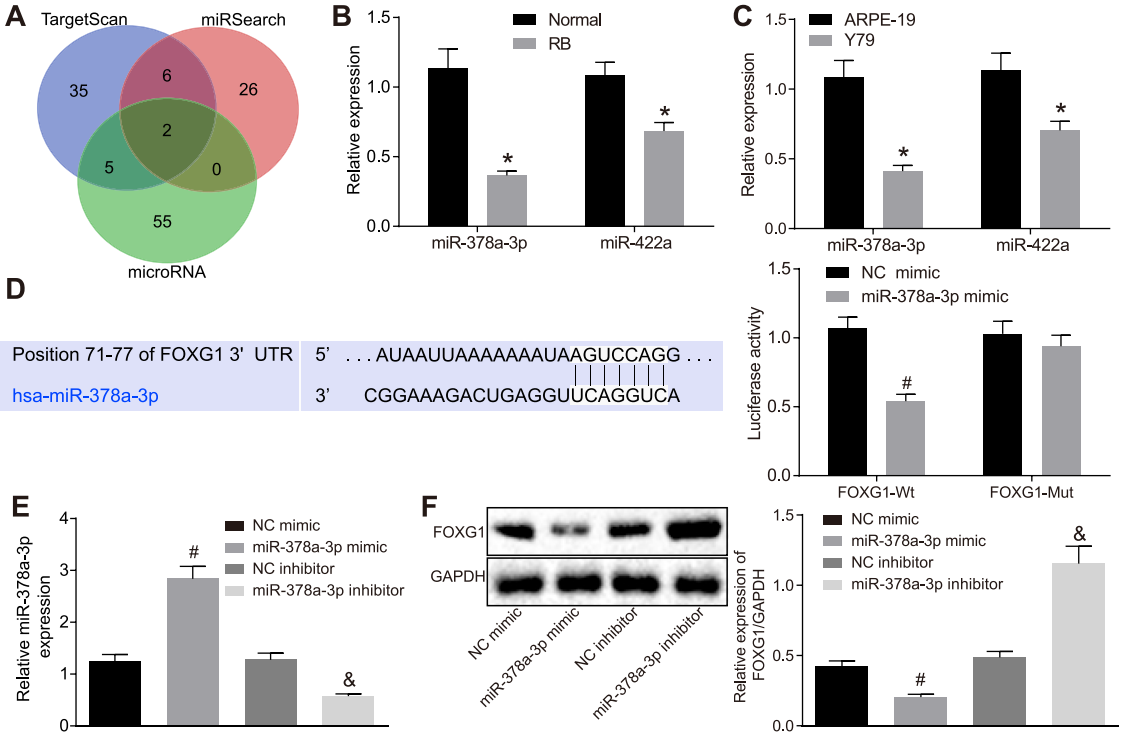

Figure 3. miR-378a-3p targets and negatively regulates FOXG1. (**A**) Prediction of regulatory miRNAs of FOXG1. The three *circles* in the figure represent the predicted results of miRNAs regulating FOXG1 in TargetScan database, miRSearch database and miRNA database, respectively, and the intersected area represents the intersected miRNAs. (**B**) The expression of miR-378a-3p and miR-422a in RB and normal tissues detected by RT-qPCR. (**C**) The expression of miR-378a-3p and miR-422a in human retinal astrocyte cell line HRA and RB cell line Y79 tested by RT-qPCR. (**D**) The binding of miR-378a-3p to FOXG1 verified by dual luciferase reporter gene assay. (**E**) The expression of miR-378a-3p after miR-378a-3p mimic and miR-378a-3p inhibitor transfection measured by RT-qPCR. (**F**) Western blot analysis of FOXG1 protein after miR-378a-3p mimic and miR-378a-3p inhibitor transfection. Statistical values were measurement data and expressed as mean ± standard deviation. Independent sample *t*-test was used for comparison of data between two groups. * $P < 0.05$ versus the normal tissues or the HRA cells. # $P < 0.05$ versus the NC mimic-transfected Y79 cells. & $P < 0.05$ versus the NC inhibitor-transfected Y79 cells. The experiment was repeated three times independently.

apoptosis rate of RB cells (Fig. 2E). These findings indicated that the downregulation of FOXG1 could contribute to the suppression of cell viability and promotion of cell apoptosis in RB.

FOXG1 Is a Target Gene of miR-378a-3p

Microarray-based gene expression profiling was performed to predict the potential mechanism of FOXG1 in RB progression. The upstream regulatory miRNAs of FOXG1 were predicted by TargetScan database, miRSearch database, and miRNA database. Two intersected miRNAs were found, namely, has-miR-422a and has-miR-378a-3p (Fig. 3A). Based on the results from the RT-qPCR, RB tissues showed significantly reduced expression of has-miR-422a and has-miR-378a-3p, in comparison with normal tissues and HRA cells, whereas the expression of has-miR-378a-3p presented with a larger fold change than that of has-miR-422a (Figs. 3B, C). The results from dual luciferase reporter gene assay displayed the decrease in the luciferase activity of FOXG1-wild type was caused upon miR-378a-3p mimic transfection, whereas the luciferase activity of FOXG1-mutant remained unaffected following miR-378a-3p mimic transfection (Fig. 3D), indicating that miR-378a-3p could bind to FOXG1. miR-378a-3p expression in RB cell line Y79 was upregulated by transfection with miR-378a-3p mimic or downregulated by transfection with miR-378a-3p inhibitor to further investigate the regulation of miR-378a-3p on FOXG1 (Fig. 3E). Subsequent Western blot analysis provided data that FOXG1 protein expression in Y79 cells transfected with miR-378a-3p mimic was notably lowered, while it was elevated when transfected with miR-378a-3p inhibitor (Fig. 3F). These findings suggest that FOXG1 could be targeted and downregulated by miR-378a-3p.

miR-378a-3p Downregulates FOXG1 to Inhibit Cell Viability and Promote Cell Apoptosis in RB

Y79 and SO-Rb50 cells were cotransfected with NC-mimic and oe-NC, miR-378a-3p mimic and oe-NC, or mir-378a-3p mimic and oe-FOXG1 to further investigate the regulatory effect of miR-378a-3p on FOXG1 and its impact on RB. The protein expression of FOXG1, Bax, Bcl-2, and CCND2 in each group was evaluated by Western blot analysis. Compared with cotransfection with NC-mimic and oe-NC, the FOXG1 expression was significantly decreased after cotransfection with miR-378a-3p mimic and oe-NC. However, the expression of FOXG1 was profoundly increased upon cotransfection with miR-378a-3p mimic and oe-FOXG1 relative to cotransfection with miR-378a-3p mimic and oe-NC (Fig. 4A, Supplementary Fig. S2A). The results from Western blot analysis demonstrated that the protein expression of Bcl-2 and CCND2 was remarkably downregulated, and the

Investigative Ophthalmology & Visual Science

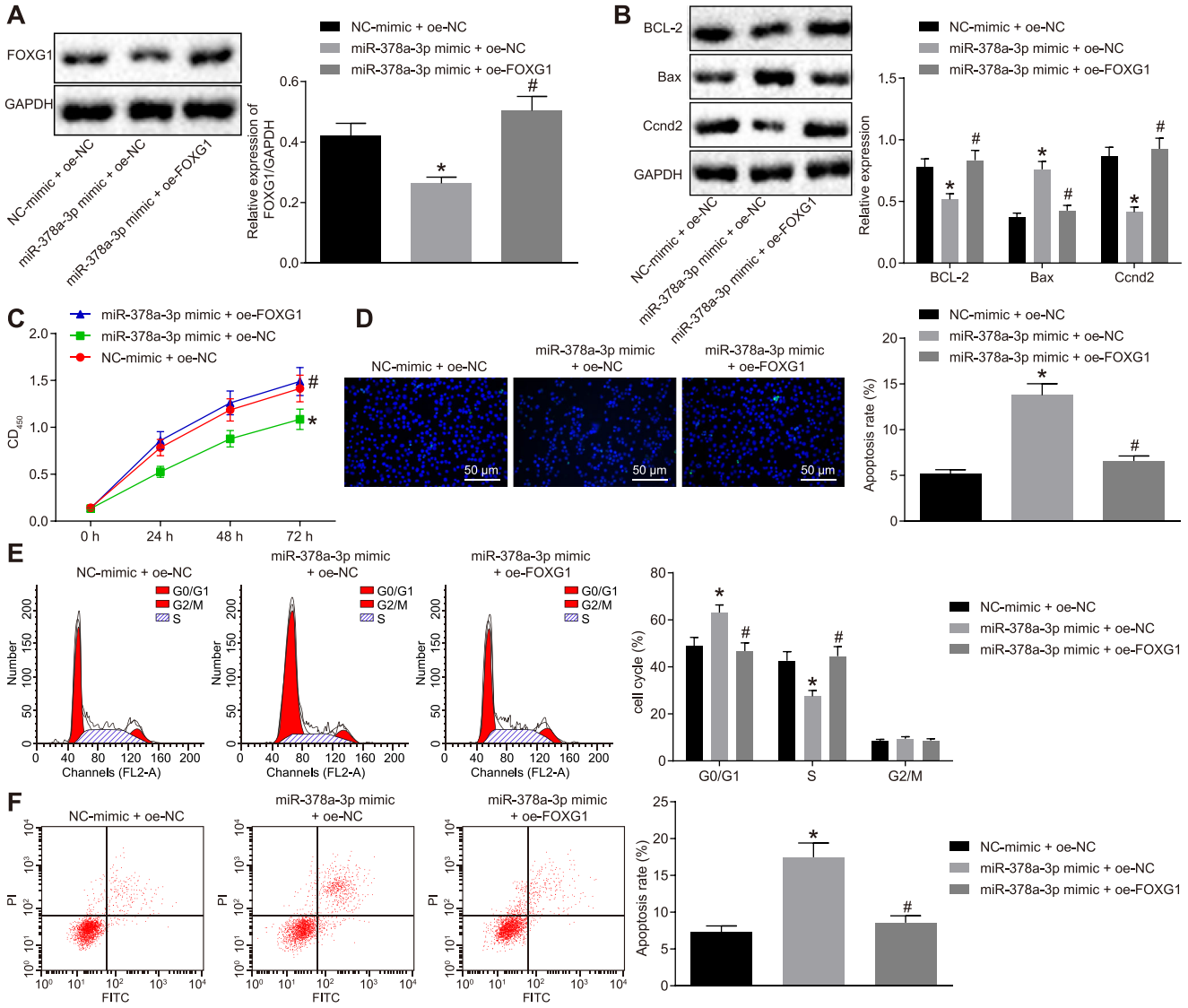

Figure 4. Upregulated miR-378a-3p results in hindered viability and promoted apoptosis of Y79 cells by inhibiting FOXG1. Y79 cells were cotransfected with NC-mimic and oe-NC, miR-378a-3p mimic and oe-NC, or miR-378a-3p mimic and oe-FOXG1. (**A**) Western blot analysis of FOXG1 protein normalized to glyceraldehyde-3-phosphate dehydrogenase (GAPDH). (**B**) Western blot analysis of Bcl-2, Bax, and CCND2 proteins normalized to GAPDH. (**C**) Cell proliferation assessed by CCK-8 assay. (**D**) Cell apoptosis measured by TUNEL assay (original magnification ×200). (**E**, **F**) Cell cycle distribution and apoptosis detected by flow cytometry. Statistical values were measurement data and expressed as mean ± standard deviation. One-way ANOVA was used for comparison of data among multiple groups, followed by a Tukey multiple comparisons post-test. * $P < 0.05$ versus Y79 cells cotransfected with NC-mimic and oe-NC. # $P < 0.05$ versus Y79 cells cotransfected with miR-378a-3p mimic and oe-NC. The experiment was repeated three times independently.

protein expression of Bax was markedly increased as a result of miR-378a-3p overexpression, all of which were reversed by overexpression of FOXG1 (Fig. 4B, Supplementary Fig. S2B). CCK-8 assay data displayed that the viability of RB cells was significantly decreased after the overexpression of miR-378a-3p, which was then reversed upon overexpression of FOXG1 (Fig. 4C, Supplementary Fig. S2C). Results of the TUNEL assay revealed a remarkable increase in cell apoptosis following miR-378a-3p elevation, while this increase induced by miR-378a-3p overexpression was decreased when the expression FOXG1 was restored (Fig. 4D, Supplementary Fig. S2D). Similar results were obtained by flow cytometry, which showed that the proportion of cells was notably increased in G0/G1 phase, then decreased in S phase, and the cell apoptosis rate was significantly increased when miR-378a-3p was elevated. However, the changes triggered by miR-378a-3p overexpression were all reversed upon upregulation of FOXG1 (Fig. 4E, Supplementary Fig. S2E). These findings showed that miR-378a-3p could restrain the cell cycle progression and promote the apoptosis of RB cells, and the overexpression of FOXG1 could reverse the inhibitory effect of miR-378a-3p on RB cells.

Elevated miR-378a-3p Delays Tumor Growth in RB In Vivo

A xenograft model was established in nude mice and tumor formation was observed and recorded to further elucidate

Investigative Ophthalmology & Visual Science

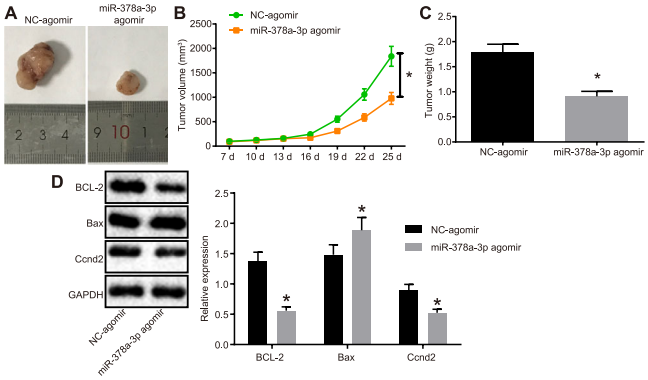

Figure 5. Restored miR-378a-3p leads to suppression of tumor growth in RB in vivo. (**A**) Xenograft tumors in nude mice after injection with NC-agomir or miR-378a-3p agomir. (**B** and **C**) Quantitative analysis of tumor volume and weight after injection with NC-agomir or miR-378a-3p agomir. (**D**) Western blot analysis of Bcl-2, Bax and CCND2 proteins in response to overexpression of miR-378a-3p normalized to glyceraldehyde-3-phosphate dehydrogenase. Statistical values were measurement data and expressed as mean ± standard deviation. Independent *t*-test was used for comparison of data between two groups. * $P < 0.05$ versus the tumor-bearing nude mice injected with NC-agomir ($n = 6$).

the effect of miR-378a-3p on RB in vivo. The results suggested that compared with the tumor-bearing nude mice injected with NC-agomir, the tumor volume and weight of tumor-bearing nude mice injected with miR-378a-3p agomir were remarkably reduced (Figs. 5A–C). The expression of Bcl-2 and CCND2 in tumor tissues from tumor-bearing nude mice detected by RT-qPCR markedly decreased, whereas the expression of Bax was significantly upregulated following the overexpression of miR-378a-3p (Fig. 5D). Thus, we concluded that miR-378a-3p overexpression could result in the inhibition of tumor growth in vivo.

Discussion

RB is the most common intraocular malignancy among children across the globe, with hereditary or nonhereditary (sporadic) malignant forms.[21] Systemic chemotherapy is the first-line therapeutic treatment, and considering the efficiency of the target tumor by systemic chemotherapy, local anticancer drug administration would be beneficial to increase the local drug concentration and minimize side effects of chemotherapy.[22] Notably, small molecules are reported to be attractive treatment targets with regard to their therapeutic significance to RB.[23,24] The present study found highly expressed FOXG1 in RB, and FOXG1 was confirmed as one target gene of miR-378a-3p. The main findings indicated that miR-378a-3p exerted an inhibitory effect on RB cell proliferation by targeting FOXG1.

The data obtained from Western blot analysis revealed an increase in FOXG1 expression in the RB tissues and cells. FOXG1, as a member of forkhead box family considered to be the key regulator of self-renewal and differentiation of neural stem cells, was also identified as one of the factors involving neurodevelopmental transcription.[25] Upregulated levels of FOXG1 was found in glioma tissues, and its upregulation was positively linked to glioma malignancy.[26] FOXG1 expression was also found to have a positive correlation with the disease progression of glioblastoma multiforme, which is one of the most common malignancies of the brain.[27] Previous research demonstrated that the decreased expression of FOXG1 inhibited the tumor growth in a xenograft mouse model of medulloblastoma.[17] The downregulation of FOXG1 has been proven to prevent the occurrence of carcinogenicity of brain tumor-initiating cells.[14] Given the importance of FOXG1 in the brain tumor glioblastoma and medulloblastoma, it was inferred that FOXG1 would also have a role in the neuronally originated RB. In the present study, downregulation of FOXG1 was found to have the ability to restrain cell growth and cell cycle entry, while promoting cell apoptosis in RB, which was consistent with previous studies.

Additionally, miRNAs have been elucidated to be functional to the clinical management of glioblastoma and medulloblastoma.[28,29] Therefore, subsequent attempts were made to explore the regulatory potential of miRNAs in RB. The results from RT-qPCR assay in our study revealed that miR-378a-3p was downregulated in RB cells. This result was in line with a previous study that showed downregulated miR-378a-3p expression in ovarian cancer,[30] as well as in CRC cells.[31] Wu et al.[32] also suggested that the ectopic expression of miR-378a-3p resulted in the inhibition of cellular proliferative and colony-forming abilities, and induced apoptosis along with G1-phase cell cycle arrest in colorectal cancer. The enforced expression of miR-378a-3p has also been shown to contribute to the reduction in cell proliferation and proliferation-associated proteins in lung cancer.[33] Similarly, accumulating data have implied that the implications of miRNAs in the progression of RB, such as miR-22-3p and miR-443,[34,35] supporting the validation of our findings. In this study, we provided evidence that enhanced miR-378a-3p could inhibit RB cell growth and induce cell apoptosis, which further supports the aforementioned tumor suppressive role of miR-378a-3p. Furthermore, miR-378a-3p role of suppressing the growth of RB cells was further confirmed by in vivo experiments.

In addition, the dual luciferase reporter gene assay data revealed that FOXG1 was a target of miR-378a-3p and negatively regulated by miR-378a-3p. FOXG1 is also reported to be regulated by other miRNAs and underlies the regulation of miRNAs in other diseases. An example of such is that miR-9 can regulate Cajal-Retzius cell differentiation and neurogenesis in telencephalon by targeting FOXG1.[36] Meanwhile, the rescue experiments in the present study suggested that elevated levels of miR-378a-3p impeded cell cycle progression and promoted cell apoptosis in RB through the downregulation of FOXG1. The overexpression of miR-378a-3p could enhance the sensitivity of breast cancer cells to tamoxifen via negatively regulating the oncogene GOLT1A.[37] miR-378a-3p could strengthen the sensitivity of ovarian cancer cells to cisplatin by targeting MAPK1/GRB2 and exerting its antitumor effect.[30] Similarly, miR-378a-3p played a role as a tumor suppressor by targeting Rab10 to slow the progression of esophageal squamous cell carcinoma.[13] All of these findings from previous studies partially supported the conclusion of our results indicating that miR-378a-3p might function as an anti-tumor miRNA in RB by targeting FOXG1.

Taken together, the key observations of our data suggested that miR-378a-3p could downregulate the expression of FOXG1, thereby restraining the cell growth and inducing cell apoptosis of RB cells. Therefore, the identification of miR-378a-3p and its potential role in mediating FOXG1 may provide insights into understanding the mechanisms and pathogenesis of RB. However, more in-depth

Investigative Ophthalmology & Visual Science

investigations are required to elucidate the specific mechanisms of miR-378a-3p that interplays with FOXG1 in the biology of RB.

Acknowledgments

We thank and appreciate our colleagues for their valuable efforts and comments on this article.

Chao Zhang and Shuai Wu designed the study. Shuai Wu collated the data, carried out data analyses and produced the initial draft of the manuscript. Chao Zhang contributed to drafting the manuscript. All authors have read and approved the final submitted manuscript.

Disclosure: **C. Zhang,** None; **S. Wu,** None

References

1. Dimaras H, Corson TW, Cobrinik D, et al. Retinoblastoma. *Nat Rev Dis Primers*. 2015;1:15021.
2. Dyer MA. Lessons from retinoblastoma: implications for cancer, development, evolution, and regenerative medicine. *Trends Mol Med*. 2016;22:863–876.
3. Benavente CA, Dyer MA. Genetics and epigenetics of human retinoblastoma. *Annu Rev Pathol*. 2015;10:547–562.
4. Aronow ME. Intra-arterial chemotherapy for retinoblastoma: experience matters but risks remain. *Ophthalmology*. 2018;125:1812.
5. Li Y, Sun W, Han N, Zou Y, Yin D. Curcumin inhibits proliferation, migration, invasion and promotes apoptosis of retinoblastoma cell lines through modulation of miR-99a and JAK/STAT pathway. *BMC Cancer*. 2018;18:1230.
6. Tabatabaei SN, Derbali RM, Yang C, et al. Co-delivery of miR-181a and melphalan by lipid nanoparticles for treatment of seeded retinoblastoma. *J Control Release*. 2019;298:177–185.
7. Li H, BB Yang. Friend or foe: the role of microRNA in chemotherapy resistance. *Acta Pharmacol Sin*. 2013;34:870–879.
8. Tan S, Wu Y, Zhang CY, Li J. Potential microRNA targets for cancer chemotherapy. *Curr Med Chem*. 2013;20:3574–3581.
9. Sage J, Ventura A. miR than meets the eye. *Genes Dev*. 2011;25:1663–1667.
10. Zhang Y, Xue C, Zhu X, Zhu X, Xian H, Huang Z. Suppression of microRNA-125a-5p upregulates the TAZ-EGFR signaling pathway and promotes retinoblastoma proliferation. *Cell Signal*. 2016;28:850–860.
11. Wang J, Wang X, Li Z, Liu H, Teng Y. MicroRNA-183 suppresses retinoblastoma cell growth, invasion and migration by targeting LRP6. *FEBS J*. 2014;281:1355–1365.
12. Velazquez-Torres G, Shoshan E, Ivan C, et al. A-to-I miR-378a-3p editing can prevent melanoma progression via regulation of PARVA expression. *Nat Commun*. 2018;9:461.
13. Ding N, Sun X, Wang T, Huang L, Wen J, Zhou Y. miR378a3p exerts tumor suppressive function on the tumorigenesis of esophageal squamous cell carcinoma by targeting Rab10. *Int J Mol Med*. 2018;42:381–391.
14. Verginelli F, Perin A, Dali R, et al. Transcription factors FOXG1 and Groucho/TLE promote glioblastoma growth. *Nat Commun*. 2013;4:2956.
15. Pancrazi L, Di Benedetto G, Colombaioni L, et al. Foxg1 localizes to mitochondria and coordinates cell differentiation and bioenergetics. *Proc Natl Acad Sci U S A*. 2015;112:13910–13915.
16. Dali R, Verginelli F, Pramatarova A, Sladek R, Stifani S. Characterization of a FOXG1:TLE1 transcriptional network in glioblastoma-initiating cells. *Mol Oncol*. 2018;12:775–787.
17. Adesina AM, Veo BL, Courteau G, et al. FOXG1 expression shows correlation with neuronal differentiation in cerebellar development, aggressive phenotype in medulloblastomas, and survival in a xenograft model of medulloblastoma. *Hum Pathol*. 2015;46:1859–1871.
18. Liu S, Yan G, Zhang J, Yu L. Knockdown of long noncoding RNA (lncRNA) metastasis-associated lung adenocarcinoma transcript 1 (MALAT1) inhibits proliferation, migration, and invasion and promotes apoptosis by targeting miR-124 in retinoblastoma. *Oncol Res*. 2018;26:581–591.
19. Xia W, Wang L, Yu D, Mu X, Zhou X. Lidocaine inhibits the progression of retinoblastoma in vitro and in vivo by modulating the miR520a3p/EGFR axis. *Mol Med Rep*. 2019;20:1333–1342.
20. Wan W, Wan W, Long Y, et al. MiR-25-3p promotes malignant phenotypes of retinoblastoma by regulating PTEN/Akt pathway. *Biomed Pharmacother*. 2019;118:109111.
21. Kamihara J, Bourdeaut F, Foulkes WD, et al. Retinoblastoma and neuroblastoma predisposition and surveillance. *Clin Cancer Res*. 2017;23:e98–e106.
22. Cocarta AI, Hobzova R, Sirc J, et al. Hydrogel implants for transscleral drug delivery for retinoblastoma treatment. *Mater Sci Eng C Mater Biol Appl*. 2019;103:109799.
23. Pritchard EM, Dyer MA, Guy RK. Progress in small molecule therapeutics for the treatment of retinoblastoma. *Mini Rev Med Chem*. 2016;16:430–454.
24. Shanmugam MK, Lee JH, Chai EZ, et al. Cancer prevention and therapy through the modulation of transcription factors by bioactive natural compounds. *Semin Cancer Biol*. 2016;40-41:35–47.
25. Bulstrode H, Johnstone E, Marques-Torrejon MA, et al. Elevated FOXG1 and SOX2 in glioblastoma enforces neural stem cell identity through transcriptional control of cell cycle and epigenetic regulators. *Genes Dev*. 2017;31:757–773.
26. Chen J, Wu X, Xing Z, et al. FOXG1 expression is elevated in glioma and inhibits glioma cell apoptosis. *J Cancer*. 2018;9:778–783.
27. Wang L, Wang J, Jin T, Zhou Y, Chen Q. FoxG1 facilitates proliferation and inhibits differentiation by downregulating FoxO/Smad signaling in glioblastoma. *Biochem Biophys Res Commun*. 2018;504:46–53.
28. Bordych C, Eisenhut M, Pick TR, Kuelahoglu C, Weber AP. Co-expression analysis as tool for the discovery of transport proteins in photorespiration. *Plant Biol (Stuttg)*. 2013;15:686–693.
29. Ajeawung NF, Li B, Kamnasaran D. Translational applications of microRNA genes in medulloblastomas. *Clin Invest Med*. 2010;33:E223–233.
30. Xu ZH, Yao TZ, Liu W. miR-378a-3p sensitizes ovarian cancer cells to cisplatin through targeting MAPK1/GRB2. *Biomed Pharmacother*. 2018;107:1410–1417.
31. Pellatt DF, Stevens JR, Wolff RK, et al. Expression profiles of miRNA subsets distinguish human colorectal carcinoma and normal colonic mucosa. *Clin Transl Gastroenterol*. 2016;7:e152.
32. Wu T, Chen W, Liu S, et al. Huaier suppresses proliferation and induces apoptosis in human pulmonary cancer cells via upregulation of miR-26b-5p. *FEBS Lett*. 2014;588:2107–2114.
33. Wang M, Sun X, Yang Y, Jiao W. Long non-coding RNA OIP5-AS1 promotes proliferation of lung cancer cells and leads to poor prognosis by targeting miR-378a-3p. *Thorac Cancer*. 2018;9:939–949.
34. Liu Y, Li H, Liu Y, Zhu Z. MiR-22-3p targeting alpha-enolase 1 regulates the proliferation of retinoblastoma cells. *Biomed Pharmacother*. 2018;105:805–812.

35. Zhang S, Gao L, Thakur A, et al. miRNA-204 suppresses human non-small cell lung cancer by targeting ATF2. *Tumour Biol*. 2016;37:11177–11186.
36. Shibata M, Kurokawa D, Nakao H, Ohmura T, Aizawa S. MicroRNA-9 modulates Cajal-Retzius cell differentiation by suppressing Foxg1 expression in mouse medial pallium. *J Neurosci*. 2008;28:10415–10421.
37. Ikeda K, Horie-Inoue K, Ueno T, et al. miR-378a-3p modulates tamoxifen sensitivity in breast cancer MCF-7 cells through targeting GOLT1A. *Sci Rep*. 2015;5:13170.

Investigative Ophthalmology & Visual Science